QUALITY ASSURANCE IN LASER-BEAM WELDING OF HEAVY SECTION STEEL SHEET

M. Dahmen*, S. Kaierle*, G. Kapper*, J. Michel**, W. Schulz*,
K. Spielvogel*, R. Poprawe*,**
*Fraunhofer-Insitut für Lasertechnik, Steinbachstraße 15, 52074 Aachen, Germany
**Lehrstuhl für Lasertechnik der RWTH Aachen, Steinbachstraße 15 52074 Aachen

Abstract

In manufacturing of welded parts which require a proof on acceptance close observation of the process is mandatory. The manufacturer is obliged to document the welding process. An approach for monitoring and recording the process of laser beam welding combining theoretical knowledge, process monitoring and welding experience will be presented. The range of application of a device for co-axial process monitoring was extended up to 20 mm sheet thickness welded in one pass at beam powers of up to 20 kW. Crucial features of the process which refer to the formation of failures were observed. The results presented give rise to the general applicability of the approach for process monitoring and recording as well as failure management.

1. Introduction

Welding applications with lasers focus mainly on the mid-section range of sheet metal and tubes. Laser powers applied range usually from 4 to 10 kW. Increasing power and sheet thickness lead to a more complex process where instabilities make the process sensitive to external and internal perturbations. Instabilities are induced due to the great input energy guided by the small Peclet number and the great aspect ratio. This will locally disturb the equilibrium of the forces maintaining the keyhole. This results in a fluctuation of the penetration depth and the formation of voids. Moreover, these instabilities may be amplified by external perturbations – e.g. fluctuations of the power density distribution or the beam power. Weld failures have a history which can be traced back to the dynamical behaviour of the keyhole by modelling the system of the interaction zone [1,2,3]. As the main indicator for the keyhole dynamics the behaviour of the absorption front was detected [4].

As tool for keyhole observation a co-axial process control (CPC) is in use which enables a spatially and temporally resolved monitoring of the capillary [5,6]. This device is approved to monitor welding processes in sheet metal with up to 6 mm thickness [7]. First aim of the work was to adopt the CPC to welding of heavy section material with a thickness of up to 20 mm requiring a maximum beam power of 20 kW. The operating principle of the sensor is based on the fact that the density of the plasma plume is optically thin compared to the plasma inside the capillary ($n_{ep}/n_{ec} \approx 1/6$). A proper observation should be possible at beam powers up to 10 kW [8]. Above this power the ratio of electron densities tends to increase, $n_{ep}/n_{ec} > 1/6$, i.e. a certain contribution of the plasma plume to the signal will occur. To assess this effect a careful calibration of the system becomes necessary. Assuming a small contribution of the plasma plume a linear increase of the signal with the penetration depth is expected.

By means of mapping the absorbing areas of the keyhole it is possible to monitor the distribution of the power density incident on keyhole front and surrounding zones. Sudden fluctuations of the power density distribution have a strong influence on the stability of the

keyhole and hence on the generation of weld failures. Therefore, the second part of the work deals with the recording of these features.

2. Experiments

The welding experiments were carried out using a fast flow CO_2 laser with an unstable resonator. It delivers a nominal output power of 20 kW. Focusing of the beam was done by a parabolic mirror made from copper characterised by a focal number of 11 and a radius of the focal spot of 0.4 mm. The focused beam has a sharp Gauss-like central peak surrounded by a diffraction ring. During the experiments of detecting the influence of the focal spot geometry a strongly mal-adjusted beam was used that was characterised by pronounced side maxima. The experimental set-up (Figure 1) consists of the focusing optics, the CPC and a lens system, a high-speed video camera in conjunction with a diode laser with a wave length of 940nm for illumination, and a clamping device. The basics of the function of the CPC are described elsewhere [5,6].

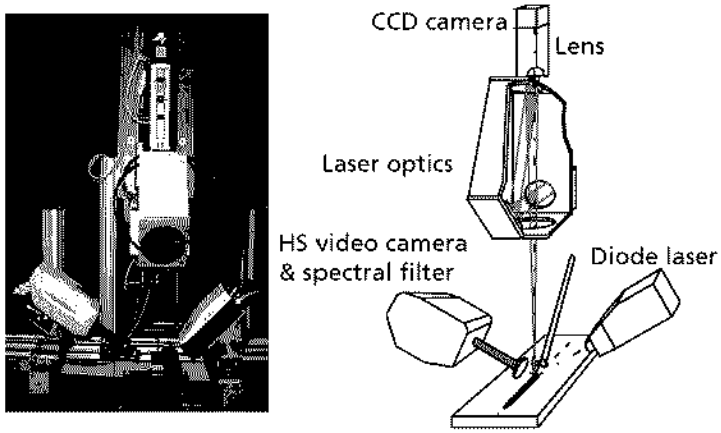

Fig. 1 Experimental set-up

The spectral range for the observation by the CPC ranged from 400 to 1100 nm. Due to the changes in plasma intensity depending on the power setting the incoming radiation was optically attenuated by neutral density filters. These filters were also used to optimise the level control of the recording. To increase the contrast on the video images an optical band-pass filter at 940±13.2 nm wave length was used. The power level of illumination was approximately 400 W in defocused mode.

Both recording systems were synchronised in order to assign video images to the images delivered by the CPC. Hereby the interpretation of the CPC images by the aid of scenes of the melt surface and the keyhole orifice is simplified.

In order to get information about the beam cross sectional area in the vicinity of the focal plane beam diagnosis were carried out. For this purpose a hollow-needle device capable to measure beams with up to 15 kW power was used.

Welding experiments were carried out as melt runs bead-on-plate. As beam parameter the power was varied between 5 and 15 kW. The relative focal position was kept constant at zero. Processing parameters changed was the feed rate that ranged from 1.0 to 8.0 m/min. The sheet thickness was changed in discrete steps $s \in \{6,12,15\}$mm.

3. Measurement of the penetration depth

Assuming the signal intensity being proportional to depth of the plasma capillary, the presentation of the signal intensity by a height profile represents the spatial 3-dimensional shape of the plasma capillary. Considering the feed as the spatial position and the shape of the plasma capillary as a moving object the superposition of all height profiles gives the minimum volume of work-piece which has been heated above melting temperature a

"capillary track" is obtained. This sampled representation allows a comparison with the spatial 3-dimensional shape of the weld seam being aware of omitting the contribution of the melt phase. By aid of this the penetration depth can be assessed. The average value for the penetration depth is calculated by two methods: firstly, the average of the track height along a fixed line in feed direction can be used for comparison with the longitudinal section along the weld; secondly, the series of maximum values of each plane vertical to the feed direction is averaged which gives the value for the penetration depth for comparison with the cross section [9].

In a preparatory step the signal of the CPC welding trials with a beam power of 10 kW were carried out. The parameter varied was the feed rate. The sheet thickness was s = 12 mm. To assess the penetration depth the seams were cross-sectioned and the penetration depth was measured at a macro section. Each value of the penetration depth represents a mean value over three sections. The results given in Figure 2 show a that the signal increases linearly with the penetration depth. At the right edge of the graph strong occur fluctuations. They are caused by the transitional behaviour of the capillary at the penetration limit.

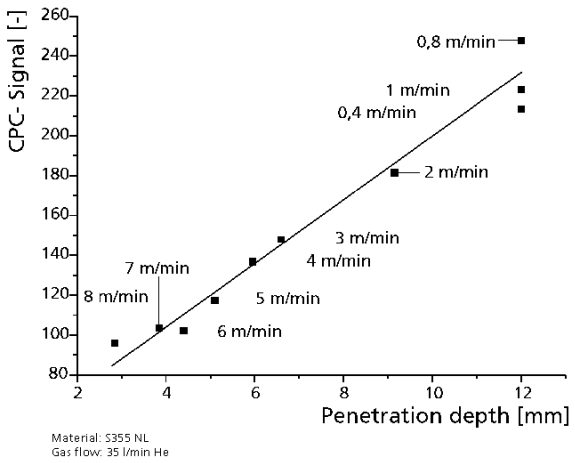

Fig. 2 Signal level dependent on the penetration depth at P_L = 10 kW

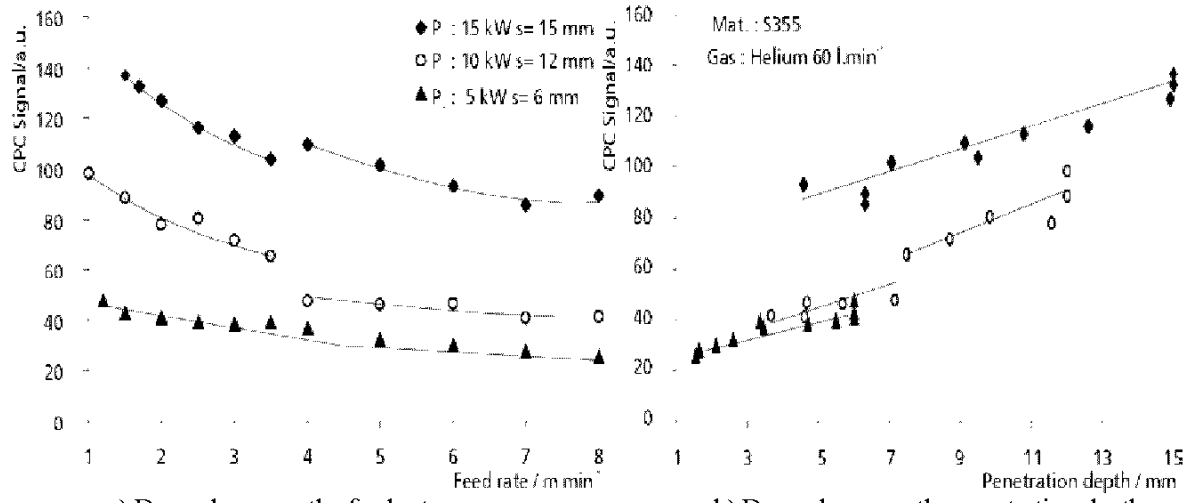

a) Dependency on the feed rate b) Dependency on the penetration depth

Fig. 3 Compiled data for different beam powers and sheet thickness

Figure 3 shows the compiled data of penetration curves for 6, 10, and 15 kW beam power at a sheet thickness of 6, 12, and 15 mm. From Figure 3a a hyperbolic trend of the CPC signal vs. the feed rate can be derived as known from "conventional" penetration curves. At 4 m/min occur a discontinuity in the graphs for 10 and 15 kW. The difference in the trend may refer to various effects, e.g. the elongation of the keyhole by a reflected beamlet (10 kW) or the occurrence of a second or higher order of reflection which tends to increase the penetration (15 kW). These results are still contradictory and need further explanation.

Plotting the signal vs. the penetration depth (Figure 3b) show the influence of the increasing beam power. The graphs for 6 and 10 kW lay almost on one straight line for a penetration depth of up to 8 mm. Above 8 mm the curve for 10 kW tends to rise a bit more progressively. This effect might be explained with a gradual increase of the electron temperature of the plasma which is confined to the keyhole. An alternative explanation might be found in the laser beam will be re-shaped by reflection at the leading edge of the capillary. Due to the different radii of curvature parts of it are focused to the bottom or the rear wall of the capillary inducing and increase of electron temperature and density which contribute to the increase of the signal. A clear offset is observed for the graph at 15 kW. This indicates that there not only the length of the plasma inside the capillary was measured. Hypothetically, a contribution of the plasma plume or a saturation of the internal plasma by scattering effects may be an explanation for this behaviour. A dependency of the signal intensity on the beam power can be observed. Fact is that the signal depends linearly on the penetration depth even for a beam power of 15 kW.

4. Controlling the geometry of the focal spot

A difficult case in quality control during laser beam welding is the surveillance of the beam properties. In the normal case the beam is monitored by a profiler off line of the manufacturing processes. Even in welding with high power lasers above 10 kW the diagnostic results are of limited significance. The surveillance by the CPC offers the opportunity to monitor the beam quality parallel by observing the interaction zone.

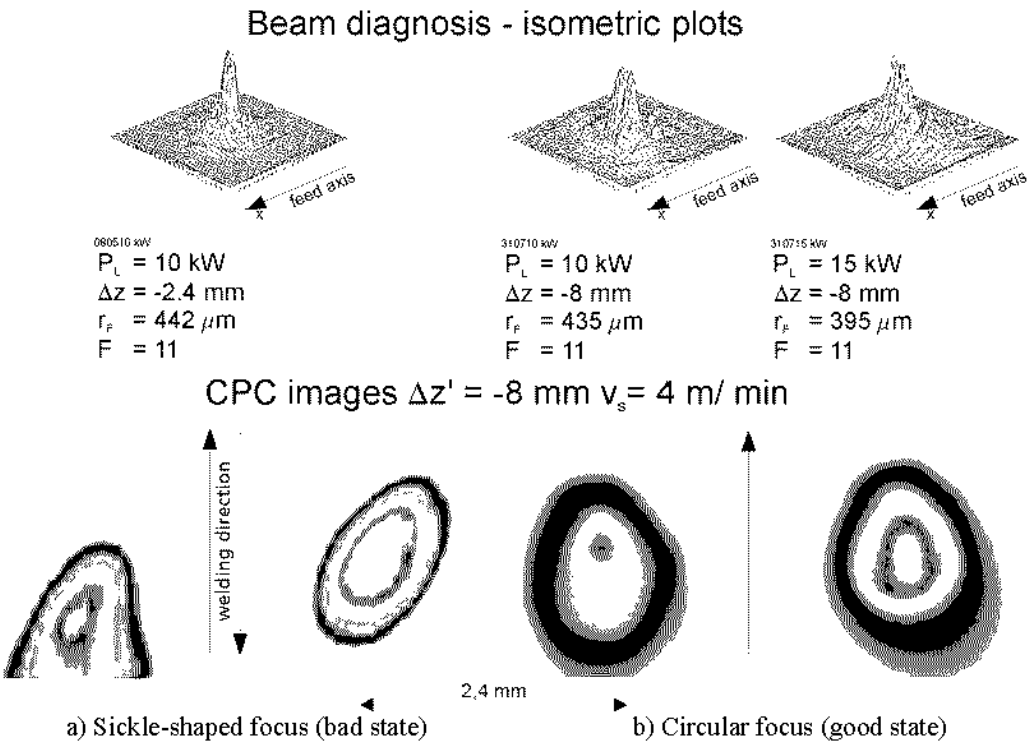

a) Sickle-shaped focus (bad state) b) Circular focus (good state)

Fig. 4 Comparison between diagnosis plots and CPC recordings

Figure 4 shows the results of experiments for two different states of adjustment of the laser resonator. The images depicted in Figure 4a were obtained by using a laser at the limit of maintenance. The optical components of the resonator were worn out with the consequence of a distorted distribution of power density and an unstable behaviour of the discharge which led

to strong fluctuations of power and intensity. The snapshot (figure 4a above) of the beam profile in the focal plane shows a asymmetric distribution with a pronounced sickle shaped secondary maximum which is clearly above the tolerated limit. In the cross-sectional view it appears as a half moon. Due to the intensity fluctuations the penetration depth of the welds varied in a range of ±15% with dislocations of the maximum penetration. Furthermore the welding result depended on the feed direction, i.e. the location of the side maximum – leading or trailing – influence the seam quality. In the lower part of Figure 4a the corresponding pattern recorded by the CPC is shown. One can easily see the action of the distorted beam profile. Depending on the direction of feed the pattern appears different. In the forward direction material is molten by the leading secondary maximum. As a consequence the contour becomes sharp-edged corresponding to the distortion of the keyhole. In reverse direction with a trailing secondary maximum the pattern is elliptical but is inclined with respect to the feed direction.

In comparison to this in Figure 4b the results for a well adjusted resonator are shown. The secondary maximum merges with the peak as shown from the diagnosis snapshot. In the CPC image the dependency on the feed direction disappears, the image is elliptical with its long axis parallel to the feed direction.

5. Visualising the keyhole shape

Of major importance for the instability of the process and the generation of failures is the shape of the keyhole. At low feed rates characterised by a Peclet number $Pe_{II} \ll 1$ the keyhole is circular. At greater Pe the absorption front becomes inclined and consequently the refection conditions are changed. By this and the melt dynamics the keyhole becomes elliptical. At increasing feed rates the elongation of the keyhole increases also. It is kept open by radiation which is reflected by the front and absorbed by the rear wall. The flow conditions are changed that failure as undercut or – in extreme cases – humping occurs.

Figure 5 shows a plot of the penetration depth vs. the feed rate for a two power levels at 10 and 15 kW and the corresponding images acquired by the CPC. The feed direction is oriented towards the top. The keyhole appears to be limited by the red areas. Its diameter lies in the order of magnitude of the diameter of the focal spot. The blue shaded area represents the molten zone.

For the position of the laser beam was kept constant from the images a nearly linear dependence or the keyhole vertex on the feed rate. If the feed rate increases the vertex is shifted backwards. The shift increases with the beam power.

At v_s = 1 m/min the keyhole is circular with a slight increase of the diameter if the power is increased from 10

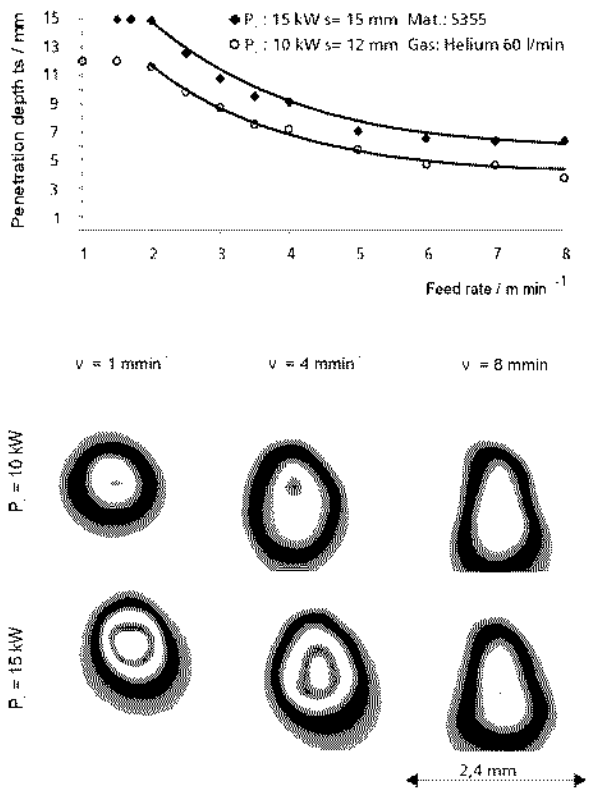

Fig. 5 Keyhole shape at various feed rates

(Pe = 1.14)to 15 kW (Pe = 1.37). If the feed rate is st to 4 m/min (Pe = 4.56 and 5.48, respectively) the orifice of the keyhole will be elongated with a peak intensity in the vicinity of the absorption front. In the upper region of the keyhole parts of the incident power are reflected and cause a egg-shaped distortion. The reflected part of the beam forms a so-called catacaustic which causes the widening of the orifice towards the back. At v_s = 8 m/min (Pe = 9.14 and 10.97, resp.) the appearance of the process is completely changed. The keyhole is strongly elongated and the locus of maximum intensity moves towards the centre of the image. Also a decrease of the maximum intensity can be observed. The keyhole may be regarded a shallow trough. As expected the upper bead of the seam is narrow and undercut. Instabilities of the process caused by the changed melt flow lead to a rough bead surface and the formation of spatters.

6. Conclusions

First results of applying a device for co-axial process control on laser beam welding of heavy section steel sheet are reported. The CPC system has been modified and tested for monitoring of long keyhole lengths. In measuring the seam depth a linear increase of the signal with the penetration depth of 10 mm at a beam power of 10 kW was found. For higher beam powers a significant contribution of the plasma plume to the level of the CPC-signal has to be taken into consideration. A discontinuity at feed rate of 4 m/min indicates also the occurrence of different orders of reflection inside the keyhole. Further experiments on clarifying

- contribution of the surface plasma on the offset of the CPC-signal
- the offset of the CPC-signal
- factors that influence the offset level, e.g. coupling conditions for the laser radiation
- spectroscopic investigations to fine an optical gap to visualise the capillary.

Trials on visualising the shape of the keyhole have shown the capability of getting information on the behaviour of the capillary at varying feed rates. Also the CPC has been proven to serve as a diagnostic tool to monitor the distribution of the power density at the boundaries of the keyhole. The results are very promising. In conjunction with modelling techniques and image processing the observability of the process as well as the data reading from the signals will be improved and the CPC will be enabled to serve as a measuring tool for on-line quality control in heavy section welding.

References

1) W. Schulz, J. Michel, M. Nießen, W. Kostrykin, P. Abels, and S. Kaierle: *Proc. LASER 2001*, München 2001, in press
2) A. Matsunawa, V. Semak: *J. Phys. D: Appl. Phys.* 30(1997), p. 798
3) R. Fabbro, K. Chouf: *Proc. ICALEO '99,* Laser Institute of America (1999), p. D 92
4) W. Schulz: *Die Dynamik des thermischen Abtrags mit Grenzschichtcharakter*, Habilitationsschrift RWTH Aachen (1998)
5) P. Abels, W. Kaierle, C. Kratzsch, R. Poprawe, W. Schulz: *Proc. ICALEO '99*, Laser Institute of America (1999), p. E 99
6) C. Kratzsch, P. Abels, S. Kaierle, R. Poprawe, W. Schulz: *Proc. AHPLA*, Osaka 1999, SPIE, p. 472
7) P. Abels, S. Kaierle, V. Kostrykin, C. Kratzsch. M. Nießen, W. Schulz: *POLICE Report 2000, Project Summary*, EU-Project No. BE 96-3562, Fraunhofer-Institut für Lasertechnik (2000)
8) M. Funk: *Absorption von CO_2-Laserstrahlung beim Laserstrahlschweißen von Grobblech*, PhD thesis, Aachen (1994)
9) G. Kapper, M. Dahmen, S. Kaierle, J. Michel, W. Schulz, D. Petring, R. Poprawe: *Proc. LASER 2001*, München 2001, in press